

Common Chaos in Arbitrarily Complex Feedback Networks

Thomas Mestl, R. J. Bagley, and Leon Glass

Department of Physiology, McGill University, 3655 Drummond Street, Montreal, Quebec, Canada H3G 1Y6

(Received 20 November 1996; revised manuscript received 15 April 1997)

A class of differential equations, which captures the logical structure of discrete time logical switching networks composed of many elements, displays deterministic chaos if each element has many inputs. Statistical features of the dynamics are approximated by using a mean field Langevin-type equation with a random telegraph signal as a stochastic forcing function, and also by considering a random walk on an N -dimensional hypercube. [S0031-9007(97)03599-0]

PACS numbers: 05.45.+b, 05.40.+j, 05.50.+q, 87.10.+e

A logical switching network is composed of logical elements that assume discrete values. Time is discrete and each element computes a logical function based on the values of inputs to that element. Logical switching networks are used to design computers [1], and as models of neural [2] and genetic networks [3]. The current work is motivated by studies of randomly generated logical networks in which the logical elements represent genes [3]. If there are a large number of elements and each element has more than two inputs, these discrete time networks show disordered behavior in which nearby trajectories diverge and cycle lengths grow exponentially as the number of elements in the network increases [3,4]. In real biological systems there are not clocking devices to generate synchronous updating, and theoretical models are more appropriately formulated as continuous differential equations [5–13]. In what follows, we analyze disordered dynamics in a differential equation analog of logical switching networks for parameter ranges that lead to disordered dynamics in the discrete system.

First consider a logical network consisting of N binary elements $\mathbf{X}(t) = (X_1(t), X_2(t), \dots, X_N(t))$, $X_i(t) = -1, +1$. The network is updated by means of the dynamical equation

$$X_i(t+1) = \Lambda_i(\mathbf{X}(t)), \quad i = 1, \dots, N, \quad (1)$$

where Λ_i is a logical function and $\mathbf{X}(t)$ is the input state at time t . We consider networks with no self-input. In other words, we assume

$$\begin{aligned} \Lambda_i(X_1, X_2, \dots, X_{i-1}, -1, X_{i+1}, \dots, X_N) \\ = \Lambda_i(X_1, X_2, \dots, X_{i-1}, 1, X_{i+1}, \dots, X_N). \end{aligned} \quad (2)$$

Λ_i generates an output of either +1 or -1 for each input state. Each Λ_i can be chosen in $2^{2^{N-1}}$ different ways, and for N fixed, there are $2^{N \times 2^{N-1}}$ different networks corresponding to Eq. (1). Thus, Eq. (1) represents the class of arbitrarily complex logical feedback networks. A K -input network is a subclass of Eq. (1) in which, for each element, the inputs are selected from $K \leq (N-1)$ inputs.

The logical structure of Eq. (1) can be captured by a differential equation [6]. For each discrete variable X_i , we associate a continuous variable x_i . The relationship

between X_i and x_i is defined as follows: $X_i = -1$ if $x_i < 0$ and $X_i = +1$ if $x_i \geq 0$. For a given set of Λ_i the differential equation

$$\frac{dx_i}{dt} = -x_i + \Lambda_i(\mathbf{X}(t)), \quad i = 1, \dots, N, \quad (3)$$

is a continuous analog of Eq. (1). For each variable, the temporal evolution is governed by a first order piecewise linear differential equation. Let $\{t_1, t_2, \dots, t_k\}$ denote the switch times when any variable of the network crosses 0. For $t_j < t < t_{j+1}$, the solution [14] of Eq. (3) for each variable x_i is

$$x_i(t) = x_i(t_j) e^{-(t-t_j)} + \Lambda_i(\mathbf{X}) [1 - e^{-(t-t_j)}]. \quad (4)$$

We carried out extensive numerical computations with $N = 64$ and the number of inputs $9 \leq K \leq 25$. For these equations, the Jacobian can be explicitly computed numerically [13]. Using the technique in [15], the leading Lyapunov number was computed. It was always positive for the randomly generated networks with $N = 64$, $9 \leq K \leq 25$, indicating deterministic chaos.

Figure 1 shows the dynamics of a single variable (lower trace) and the forcing function for that variable (upper trace) $\xi(t) = \Lambda_i(\mathbf{X}(t))$ from Eq. (3).

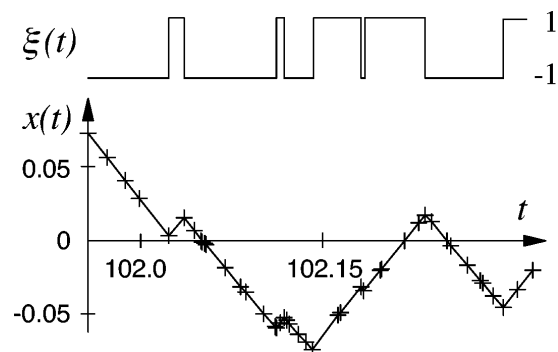


FIG. 1. Dynamics in a system with $N = 64$, $K = 20$ showing fluctuation of a single variable x (lower trace) and its associated forcing function (upper trace) $\xi(t) = \Lambda_i(\mathbf{X}(t))$ from Eq. (3). Each zero crossing of any variable is designated by a +. Because of the short times between switches, the piecewise exponential trajectory appears as straight line segments.

In Eq. (3) each variable experiences a fluctuating field described by a Langevin-type differential equation

$$\frac{dx}{dt} = -x + \xi(t). \quad (5)$$

Here, however, $\xi(t)$ is not a random variable, but rather it is a chaotic fluctuating variable switching back and forth between ± 1 as the deterministic trajectory crosses thresholds in N -dimensional state space.

The fluctuating forcing function in Fig. 1 (upper trace) is suggestive of the random telegraph signal (RTS)—a signal that switches randomly between the two values ± 1 [16,17]. The usual assumption is that the time between switches is Poisson distributed with mean switch time τ .

Equation (5) when $\xi(t)$ is the RTS has been previously analyzed [17]. The autocorrelation function $C_x(t)$ is

$$C_x(t) = \frac{1}{1 - \frac{2}{\tau}} \left(e^{-(2/\tau)|t|} - \frac{2}{\tau} e^{-|t|} \right), \quad (6)$$

and the power spectrum is

$$S(f) = \frac{1}{2\pi\tau[(2\pi f)^2 + 1][(2\pi f)^2 + (\frac{2}{\tau})^2]}. \quad (7)$$

The density of x is

$$\rho(x) = c|1 - x^2|^{(1/\tau)-1}, \quad |x| \leq 1, \quad (8)$$

with c a normalization constant determined by $\int_{-1}^{+1} \rho(x) dx = 1$ [18].

These results provide an approximate theory for the deterministic differential equation. Figure 2(a) shows a time series of a single variable x_i in a network with $N = 64$, $K = 20$, together with the corresponding density distribution Fig. 2(b), power spectrum Fig. 2(c), and distribution of times τ_i between switching in the forcing $\xi(t)$, Fig. 2(d). Superimposed on these results are the analytic results found for Eq. (5) (dashed lines), but with the assumption that $\xi(t)$ is the RTS with the same mean time between switches as in the deterministic equation.

There are several differences between the two results. The density of intervals of a Poisson process is exponential with equal values for the mean and the standard deviation. In the deterministic equation, the density distribution for times between switches, $\rho(\tau_i)$, has a higher density for short and long times, Fig. 2(d), than the exponential function. The mean time between switches is 0.041 85 with standard deviation 0.052 17. The deterministic system gives a broader density distribution, $\rho(x)$ Fig. 2(b), than the stochastic model. However, despite these differences, Eq. (5) with $\xi(t)$ given by an appropriate RTS provides a reasonable first approximation to the dynamics in Eq. (3).

We now consider the relationship between the mean time between switches of the forcing function in Eq. (5) and the mean zero crossing times of x . We designate the mean time between switches and zero-crossing time

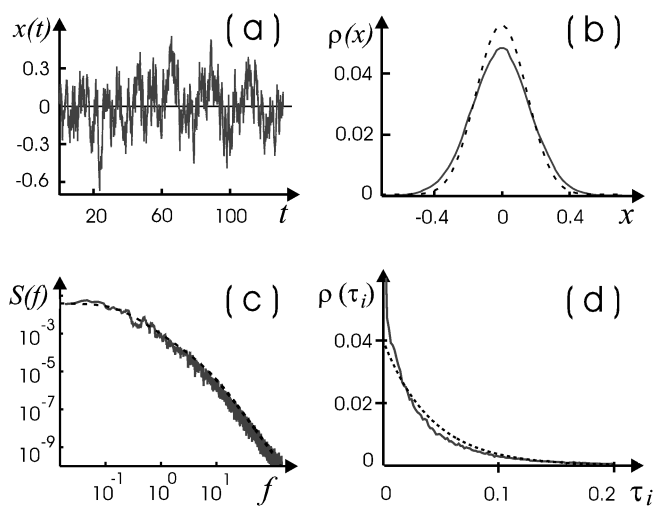


FIG. 2. Dynamics over 20000 switch times ($N = 64$, $K = 20$) compared with results from Eq. (5) with the RTS as stochastic forcing. The theoretical results for the RTS forcing are shown as dashed lines. In the RTS model we take $\tau = 0.04185$ to correspond to the numerically determined mean value in the deterministic equation. (a) A typical variable, x_i in the deterministic system. (b) Density distribution $\rho(x_i)$ averaged over all i , with 100 bins in the interval $[-1, 1]$, theoretical result from Eq. (8). (c) The power spectrum. The theoretical result from Eq. (7) is obscured under the numerically determined power spectrum. (d) Distribution $\rho(\tau_i)$ of times τ_i between switching in the forcing $\xi(t)$.

for the RTS forcing by τ and t_z , respectively. The corresponding quantities for the deterministic system are given by $\bar{\tau}$ and \bar{t}_z .

In Eq. (5) with the RTS as the forcing signal, if $\tau \gg 1$ then x will cross zero almost every time $\xi(t)$ switches, so that $t_z \approx \tau$. We are not aware of analytic results for smaller values of τ . In Fig. 3(a) the + represent numerical results and the solid curve is

$$t_z = \sqrt{\pi\tau}. \quad (9)$$

There is close agreement for sufficiently low values of τ , but we have no derivation.

Now consider the deterministic system. If we assume that the logical function Λ_i combines K inputs randomly, a switch in the forcing of any given variable will occur with a probability of $\frac{K}{2(N-1)}$ whenever any other variable crosses its threshold. For a given time length T sufficiently long, the average number of expected zero crossings for a single variable is $n_z = \frac{T}{\bar{t}_z}$. The total number of zero crossings for all variables is $n_z N$. Consequently, the expected number of switches of the forcing function for a given variable in time T is $\frac{n_z N K}{2(N-1)}$, which should equal $T/\bar{\tau}$. Consequently, for large N we obtain

$$\bar{t}_z = \frac{K}{2} \bar{\tau}, \quad (10)$$

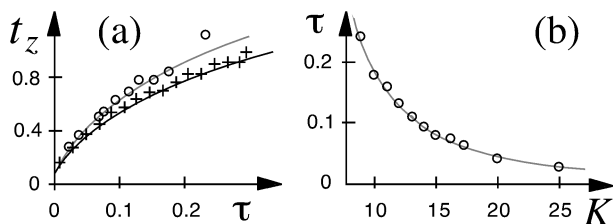


FIG. 3. (a) The mean zero crossing time t_z in the RTS model as a function of τ (+), based on the mean of 5,000 zero crossings for several values of τ . The data are well described by $t_z = (\pi\tau)^{1/2}$, which is completely covered by the data points (+). The circles (o) are computations from Eq. (3) fitted by the curve $2.13\tau^{1/2}$. (b) $\bar{\tau}$ as a function of K , compared with numerical data (o) fitted by Eq. (11) $\tau(K) = \frac{18.1}{K^2}$.

which agrees with the numerical computations. The values for \bar{t}_z and $\bar{\tau}$ are plotted in Fig. 3(a). Taking our cue from the system with RTS forcing, the data fall approximately on the curve $\bar{t}_z = c\sqrt{\pi\bar{\tau}}$ where $c \approx 1.2$. This expression is consistent with Eq. (10), provided

$$\bar{\tau} = \frac{4\pi c^2}{K^2}. \quad (11)$$

Figure 3(b) compares $\bar{\tau}$ as a function of K from the numerical simulations with Eq. (11).

The above arguments lead us to conjecture that the statistical features of the chaotic dynamics in Eq. (3) for sufficiently large K and N depend on the number of input variables K rather than the dimension of the network.

Now we adopt a more global perspective. A solution trajectory of Eq. (3) can be represented symbolically by a sequence of logical states $\{\mathbf{X}_1, \mathbf{X}_2, \dots, \mathbf{X}_k\}$ that are encountered when starting from some arbitrary initial condition. The Hamming distance h , $0 \leq h \leq N$, between two logical states is the number of coordinates in which the two states are different [3]. Since each logical state is a Hamming distance of one from the preceding state, the dynamics can be represented schematically by a walk on an N -dimensional hypercube (N -cube) where at each step there is a transition to a neighboring vertex [19]. In order to compare networks of different dimension, it is useful to define the *normalized* Hamming distance H ,

$$H = \frac{h - \frac{N}{2}}{\frac{N}{2}}. \quad (12)$$

For any two vertices on an N -cube, $0 \leq |H| \leq 1$.

In the deterministic equations, there are restrictions on the allowed transitions imposed by the structure of the network, but we simply consider a random walk on an N -cube. Let $p(h, n)$ denote the probability that the Hamming distance from some arbitrary starting vertex is h after n steps. Then $p(h, n)$ satisfies the recursion relation

$$p(h, n) = p(h-1, n-1) \frac{N-(h-1)}{N} + p(h+1, n-1) \frac{h+1}{N}, \quad (13)$$

where $\frac{N-(h-1)}{N}$ and $\frac{h-1}{N}$ give the probabilities of increasing and decreasing, respectively, the Hamming distance on any given step. Based on the above, the normalized Hamming distance, Eq. (12), is

$$H(n) = \frac{N-2}{N} H(n-1) = \left(\frac{N-2}{N}\right)^n, \quad (14)$$

where $H(0) = 1$, $n \geq 0$. Thus, the random walk on the N -cube leads to an exponential decay of $H(n)$ to 0 [20]. However, this is not the case in the deterministic equation, Fig. 4. For the deterministic system, $H(n)$ is well described by a stretched exponential of the form

$$H(n) = \exp^{-(n/n_0)^\beta}. \quad (15)$$

Stretched exponential relaxation has been widely observed in a variety of physical and biological settings [21]. Two factors may contribute to the nonexponential decay in the current situation: (i) Following a zero crossing, the corresponding variable will remain in the neighborhood of zero for several integration steps and will therefore have an increased probability for zero crossing so that Eq. (13) does not hold; (ii) restrictions are imposed by the logical network since each edge can only be traversed in one orientation [19]. The relative importance of these factors needs further investigation.

Equation (3) is a differential equation modeling complex networks with a definite logical structure. Early research which investigated this equation, or equations with similar structure, analyzed conditions for steady states and limit cycles [5–8]. Although deterministic chaos has also been observed in related models of neural and gene networks [9–13], there is no general theory. Our approach is related to earlier criteria for chaotic dynamics in Hopfield-type neural networks [10]. In this earlier work, a Langevin-type equation was derived in which the forcing term was Gaussian noise rather than the RTS.

Biological systems are often modeled by feedback networks of great complexity. An unresolved issue is

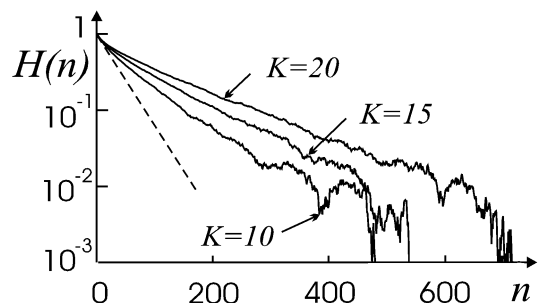


FIG. 4. Semilog plot of the normalized Hamming distance H for different values of K as a function of n (averaged over 10 different networks with 50 initial conditions each, $N = 64$). The dashed line gives the falloff derived from a random walk on the hypercube Eq. (14). $H(n)$ is well described by a stretched exponential, Eq. (15): $K = 10$, $n_0 = 53.6$, $\beta = 0.828$; $K = 15$, $n_0 = 69.4$, $\beta = 0.784$; $K = 20$, $n_0 = 88.9$, $\beta = 0.760$.

whether the dynamics described here might reflect normal function and behavior, or whether network connectivity and structure are selected to lead to a more orderly dynamics.

This research has been supported by grants from NSERC and FCAR. Thomas Mestl thanks NATO for partial support directed through the Norwegian Research Council.

-
- [1] W. Keister, A. E. Ritchie, and S. H. Washburn, *The Design of Switching Circuits* (D. Van Nostrand, Toronto, 1951); S. H. Unger, *The Essence of Logic Circuits* (IEEE Press, Piscataway, New Jersey, 1997), 2nd ed.
- [2] W. S. McCulloch and W. Pitts, *Bull. Math. Biophys.* **5**, 115 (1943); J. J. Hopfield, *Proc. Natl. Acad. Sci. U.S.A.* **79**, 2254 (1982).
- [3] S. A. Kauffman, *J. Theor. Biol.* **22**, 437 (1969); S. A. Kauffman, *Origins of Order: Self-Organization and Selection in Evolution* (Oxford University Press, Oxford, 1993).
- [4] B. Derrida and Y. Pomeau, *Europhys. Lett.* **1**, 45 (1986); B. Derrida and Y. Pomeau, *Europhys. Lett.* **2**, 739 (1986); B. Luque and R. V. Solé, *Phys. Rev. E* **55**, 257 (1997).
- [5] S. Grossberg, *Proc. Natl. Acad. Sci. U.S.A.* **58**, 1329 (1967).
- [6] L. Glass, *J. Chem. Phys.* **63**, 1325 (1975); L. Glass and J. Pasternack, *J. Math. Biol.* **6**, 207 (1978).
- [7] J. J. Hopfield *Proc. Natl. Acad. Sci. U.S.A.* **81**, 3088 (1984).
- [8] R. Thomas and R. D. Àri, *Biological Feedback* (CRC Press, Boca Raton, 1990); T. Mestl, E. Plahte, and S. W. Omholt, *J. Theor. Biol.* **176**, 291 (1995); T. Mestl, E. Plahte, and S. W. Omholt, *Dyn. Stab. Syst.* **2**, 179 (1995).
- [9] K. E. Kürten and J. W. Clark, *Phys. Lett.* **114A**, 413 (1986); T. B. Kepler, S. Datt, R. B. Meyer, and L. F. Abbott, *Physica (Amsterdam)* **46D**, 449 (1990).
- [10] H. Sompolinsky, A. Crisanti, and H. J. Sommers, *Phys. Rev. Lett.* **61**, 259 (1988).
- [11] J. E. Lewis and L. Glass, *Int. J. Bifurcation. Chaos and Sci. Eng.* **2**, 477 (1991); J. E. Lewis and L. Glass, *Neural Comput.* **4**, 621 (1992). These papers demonstrate that the Hopfield model [7,10] is a subclass of Eq. (3) if the sigmoidal function in the Hopfield model goes to a step function and if $\Lambda_i(\mathbf{X})$ can assume any value depending on its logical state.
- [12] P. K. Das II, W. C. Schieve, and Z. Zeng, *Phys. Lett. A* **161**, 60 (1991); J. E. Moreira and J. S. Andrade, Jr., *Physica (Amsterdam)* **206A**, 271 (1994).
- [13] T. Mestl, C. Lemay, and L. Glass, *Physica (Amsterdam)* **98D**, 35 (1996).
- [14] In general, for each i , $x_i(t) = 0$ only at isolated values of t , and there is no time for which $x_i(t) = x_j(t) = 0$, $i \neq j$ [6].
- [15] E. Ott, *Chaos in Dynamical Systems* (Cambridge University Press, Cambridge, England, 1993), Chap. 4.
- [16] G. W. Kenrick, *Philos. Mag.* **7**, 176 (1929); S. O. Rice, *Bell Syst. Tech. J.* **23**, 282 (1945); S. Machlup, *J. Appl. Phys.* **3**, 341–343 (1954); Y. Wang, *J. Appl. Phys.* **74**, 15 (1993). The autocorrelation function of the RTS is an exponential function and the power spectrum is $S_{\text{RTS}}(f) = \frac{1}{2\pi\tau} \frac{1}{(2\pi f)^2 + (2/\tau)^2}$.
- [17] C. W. Helstrom, *Probability and Stochastic Processes for Engineers* (Collier Macmillan, Toronto, 1990).
- [18] W. M. Wonham and A. T. Fuller, *J. Electron. Control* **4**, 567 (1958); W. Horsthemke and R. Lefever, *Noise-Induced Transitions: Theory and Applications in Physics, Chemistry, and Biology* (Springer-Verlag, Berlin, 1984).
- [19] In the differential equation, the coordinate axes subdivide the state space into 2^N orthants, where each orthant is labeled with the N -vector \mathbf{X} . The logical states \mathbf{X} thus identify vertices of an N -cube in which each vertex is adjacent to N vertices that differ only in one locus. For Eq. (3), the associated logical network in Eq. (1) defines a directed graph on the N -cube in which each edge has unique orientation corresponding to the allowed flows in the analogous equation (3) [6].
- [20] The same Markov model arises in the analysis of diffusion in a central force field, and the Ehrenfest urn model in which balls are randomly removed from one of two urns and placed in the other, P. Ehrenfest and T. Ehrenfest, *Phys. Z.* **8**, 311 (1907); K. W. F. Kohlrusch and E. Schrödinger, *Phys. Z.* **27**, 306 (1926); M. C. Wang and G. E. Uhlenbeck, *Rev. Mod. Phys.* **17**, 323 (1945); M. Kac, *Am. Math. Monthly* **54**, 369 (1947); W. Feller, *An Introduction to Probability Theory and Its Applications* (John Wiley & Sons, London, 1966), Vol. 1, p. 343.
- [21] J.-M. Flesselles and R. Botet, *J. Phys. A* **22**, 903 (1989); J. B. Bassingthwaite, L. S. Liebovitch, and B. J. West, *Fractal Physiology* (Oxford University Press, New York, 1994); B. D. Hughes, *Random Walks and Random Environments* (Clarendon Press, Oxford, 1995), Vol. 1.